Journal of Solid-Phase Biochemistry, Vol. 3, No. 4, 1978

ANALYSIS OF THE REACTION KINETICS OF SINGLE ESTERASE SEPHAROSE BEADS BY MICROFLUOROMETRY OF THE FLUOROGENIC SUBSTRATE TURNOVER[1]

OTTO HANNIBAL-FRIEDRICH[2] and MANFRED SERNETZ[3]

Institut für Biochemie und Endokrinologie, FB 18
Frankfurter Strasse 100, D-6300 Giessen, Germany

Accepted December 20, 1978

Heterogeneous catalysis of esterase (E.C. 3.1.1.1) immobilized on CNBr-Sepharose 4B was analyzed by microfluorometry. The hydrolysis of fluorescein diacetate was measured within single esterase-Sepharose beads during steady-state turnover. Fluorescence intensity profiles, total intensities, and reaction rates of single beads were measured by means of a microfluorometer. Their suitability for determining the kinetic constants of the system was evaluated by comparison with the theoretical values of the kinetic model. The computation was based on the kinetic equations describing the interaction of internal diffusion and enzymatic reaction with noncompetitive product inhibition within spherical particles. A method is described which can be used to derive the true K_m of the immobilized enzyme from a correlation of intensity- and turnover-dependent apparent K_m's. Effectiveness factors and Damköhler numbers for individual esterase-Sepharose beads were determined from relative total fluorescence intensities and fluorescence intensity profiles, respectively.

INTRODUCTION

Kinetic equations describing the heterogeneous catalysis of immobilized enzymes in spherical particles have been given by Lasch (1), Köstner (2), Regan (3), and Horvath (4). It had been characteristic of all previous attempts that the postulated kinetic features and laws, which had been derived for catalytically active particles, could not be examined experimentally on the single particles themselves, but only served as a basis for the calculation of the kinetic behavior and performance of reactors.

Several attempts, however, have been made to visualize at least the enzyme distribution (5) and the site of enzyme reaction within single beads (6). The present investigation is based on an experimental technique suggested by Sernetz et al. (7,8). Kinetic parameters derived directly from

[1]This investigation was supported by grant Se 315/4 of the Deutsche Forschungsgemeinschaft.
[2]Present address: Battelle-Institut e.V., Am Römerhof 35, 6000 Frankfurt/Main 90.
[3]Correspondence should be addressed to: M. Sernetz, Institut für Biochemie und Endokrinologie, FB 18, Frankfurter Strasse 100, D-6300, Giessen.

0146-0641/78/1200-0301$03.00/0

the data obtained by microfluorometry of the turnover of fluorogenic substrates in single enzyme-Sepharose beads. Its aim is to define suitable microfluorometric parameters for the evaluation of the kinetic constants of the system.

MATERIALS AND METHODS

The main characteristics of the method and instrumentation have been described previously (7,8); therefore, only instrumental improvements are reported here. More details are given in (9). The microscope fluorometer (Zeiss-Universal) was equipped with an incident-light condenser RS III, a photometer head MPM-Zeiss, a variable measuring field diaphragm, a photomultiplier EMI 6256 B, and a stabilized xenon high-pressure lamp XBO 150 W. An additional variable rectangular illumination field diaphragm (Leitz) was introduced into the incident light field plane.

The spectral response was selected by excitation filters BG 12 (3 mm) and BG 38 (3 mm), a dichromatic mirror FT 510, and barrier filters OG 50 and RG 65 (Zeiss). A neofluar 16/0.40 (Zeiss) objective was used. For scanning, a low-gear synchronous motor was coupled directly to the microscope stage drive. The wedge-shaped flow chamber (8) was improved (9) by cementing a glass slide onto an alloy frame with oblique drillings. The cover glass was sealed with an elastic impression material (Xantopren (R), Bayer). The substrate was perfused at 60–90 ml/h by means of a peristaltic pump (Minipuls, Gilson), operating almost free of pulsation and of a high, constant speed. Thus, laminar flow velocities of about 3 cm/sec were established in the flow chamber. This yielded turnover rates independent of the pumping speed. Comparative spectrofluorometry was performed with a Perkin Elmer 204 spectrofluorometer and a Zeiss PMQ II-ZMF 4 fluorometer (excitation Hg 365 nm, with the emission monochromator set to 520 nm).

Pig liver esterase (E.C. 3.1.1.1), mol. wt. 180,000, was supplied by Boehringer Mannheim. For fluorometric assays of the free enzyme it was dialyzed against a 0.133 M phosphate buffer of pH 7.0 and diluted to a protein content of 50 mg/l. To prepare 10^{-2} mol of a stock solution fluorescein-diacetate (FDA) (NBC) was dissolved in 0.1 l acetone p.a. (Merck) (10); this was further diluted in phosphate buffer to 10^{-7}–10^{-5} mol/l immediately before use. The acetone concentration was kept constant at 5% in all assays (9). The reactions were started by the addition of 100 µl enzyme solution to 3 ml substrate solution.

The Michaelis constant of the free esterase for FDA was determined to be $K_m \approx 3 \times 10^{-5}$ M, the maximum velocity at pH 7.0 was found to be $V_{max} \approx 54$ mol sec^{-1}/mg enzyme, corresponding to a molar catalytic activity of about 12 sec^{-1} (9). The product fluorescein acts as a noncompetitive

inhibitor by unspecific binding to the enzyme. For inhibition experiments, solutions of fluorescein sodium (Merck) were calibrated against fluorescein resulting from alkaline or enzymatic hydrolysis of FDA. The inhibition constant was determined as $K_I = 7.5 \times 10^{-6}$ mol/l (9).

The esterase was immobilized (9) on CNBr-activated Sepharose 4B (Pharmacia) (0.2–8 mg/g Sepharose). To study the enzyme binding to the carrier, the esterase-Sepharose beads were labelled with fluorescein-isothiocyanate (FITC). The FITC fluorescence of single beads was measured as described for the turnover measurements. A microscope interferometer (Micro–Mach–Zehnder, Leitz) was used for the microrefractometric determination of the homogeneity of the gel concentration within the individual beads and its variation between different beads of a suspension.

RESULTS AND DISCUSSION

Theoretical Considerations

For the description of the interaction of internal diffusion and enzymatic reaction in spherical particles, the following assumptions corresponding to the experimental conditions in our system (see below) have been taken into account (11):

1. The enzyme is distributed homogeneously within the matrix.
2. There is no binding or only concentration-proportional binding between matrix and substrate or product.
3. There are no electrostatic effects due to insufficient buffer capacity.
4. High flow velocity relative to the particles prevents formation of external stagnant diffusion layer.
5. The reaction runs isothermally; the pressure drop within the porous material is negligible.
6. Substrate and product are transported within the carrier by diffusion only.
7. All observations are performed in the steady state: $ds/dt = dp/dt = 0$.

If we assume internal diffusion to be governed by Fick's 2nd law and enzyme catalysis to follow Michaelis–Menten kinetics under the special extension of noncompetitive product inhibition, and if we define the dimensionless relative coordinates as

$$s = \frac{S}{S_a}, \qquad p = \frac{P}{S_a}, \qquad j = \frac{J}{S_a}, \qquad r = \frac{r'}{R} \qquad (1)\text{–}(4)$$

and the parameters as

$$\alpha = \frac{S_a}{K_m}, \qquad \beta = \frac{K_m}{K_j} \cdot \frac{D_s}{D_p} \tag{5),(6}$$

the known fundamental kinetic equation describing the substrate concentration profiles can be written as

$$\frac{d^2s}{dr^2} + \frac{2}{r} \cdot \frac{ds}{dr} = \frac{\sigma \cdot s}{(1+\alpha s)[1+\alpha\beta(1-s)]} \tag{7}$$

using the mass balance

$$j = p = (1-s)D_s/D_p \tag{8}$$

where

s, p, j = dimensionless substrate, product, and inhibitor concentrations
S, P, J = concentrations within the bead
S_a = given substrate concentration outside the bead
K_m, K_I = Michaelis and inhibitor constants
D_s, D_p = diffusion constants
α = relative substrate concentration
β = effective inhibitor constant
r, r' = dimensionless radial coordinate, radial coordinate
R = bead radius
σ = Damköhler number

The Michaelis constant K_m of the immobilized enzyme may be different from that of the free enzyme due to microenvironmental influences and conformational changes of the bound enzyme. The effective inhibitor constant β is defined as the relation of the true constants weighted by the relation of the diffusion constants. In case of $K_I = \infty$ or $\beta = 0$, Eq. (7) simplifies to the unihibited case (11)

$$\frac{d^2s}{dr^2} + \frac{2}{r}\frac{ds}{dr} = \frac{\sigma \cdot s}{1+\alpha s} \tag{9}$$

The Damköhler number σ (12)

$$\sigma = \frac{V_m \cdot R^2}{K_m \cdot D_s} \tag{10}$$

or its square root $\tau = \sigma^{1/2}$, the Thiele modulus (13), is the only parameter describing the kinetic properties of the system, besides the ratio of the diffusion constants D_s/D_p and the known external concentrations given by the experimental conditions.

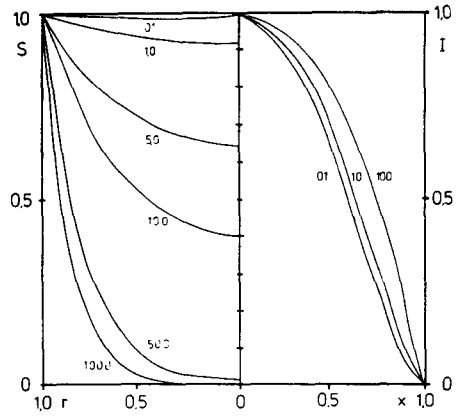

FIG. 1. Radial concentration profiles S of substrate (left) and relative fluorescence profiles I of product (right) for substrate concentration $\alpha = 1$, with Damköhler number σ as parameter.

Since there are no analytical solutions to Eq. (7), numerical methods using standard 4th-order Runge-Kutta programs had to be applied. The initial condition $s_{(r=0)}$ was evaluated iteratively according to a method by Lasch (1). Figure 1 shows the substrate concentration profiles and the product fluorescence intensity profiles as a function of the radius. Figure 2 gives the substrate concentration in the center of the sphere as a function of σ, both without and with noncompetitive inhibition ($\beta = 4$). Figures 1 and 2 indicate that only for Damköhler numbers in the range of $0.5 < \sigma < 200$ the substrate concentration profile deviates significantly from the following two limiting cases: $s = 1$ for all r, no diffusional limitation; and $s = 1$ for $r = 1$, $s = 0$ for $r < 1$, pure diffusional limitation. Figure 2 demonstrates the antagonism between diffusion limitation and chemical inhibition, as described in the literature (14,15).

Due to the complementarity of substrate and product concentration, as described by the mass balance (Eq. 8) in the case of pure diffusional limitation, the product is distributed homogeneously over all the matrix, i.e., p is constant for $r < 1$. This is achieved, e.g., by high enzyme concentrations; thus, enzymatic reactions are practically limited to the surface of the sphere. This case was reported by Sernetz et al. (7), but misinterpreted as a case without diffusional limitation due to the assumption of proportionality between substrate and product. Because of the complementarity of substrate and product concentrations (Eq. 8), only cases of diffusional influence (see Fig. 2) can lead to an accumulation of product within the matrix and thus to its experimental detectability by the method described.

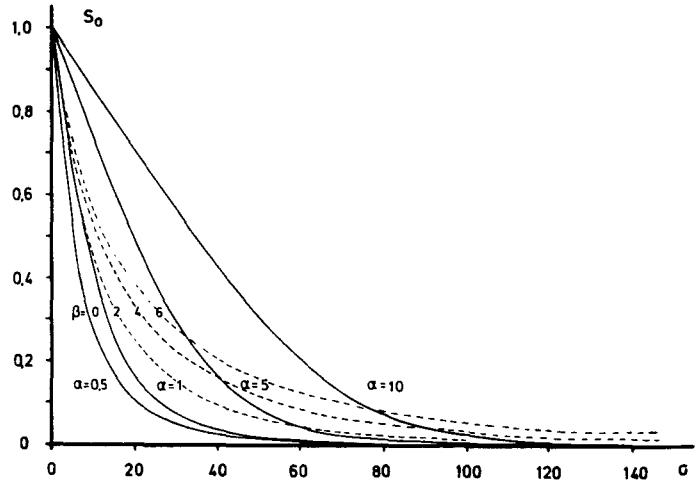

FIG. 2. Substrate concentration S in the center of a sphere as a function of the Damköhler number σ, with the concentration α (———) and the degrees of inhibition β (– – –) as parameters.

The apparent free product concentration p within the matrix can be modified (a) by proportional binding of the product to the matrix and (b) by a change of quantum yield due to the binding. Both lead to a proportional change of the concentration of the product by a factor B at any point of the sphere; thus

$$p = B(1-s)D_s/D_p \tag{11}$$

For all integrations B can be included into the proportionality constants k_i, which were set $k_i = 1$ in all model calculations (see below).

Theoretically, there are three possible experimental ways to look at the fluorescence of the product formed by a single immobilized enzyme-matrix bead, provided that the condition of direct proportionality between fluorescence intensity I and product concentration p can be verified experimentally (8):

$$I = I_0 \cdot \phi \cdot \varepsilon \cdot p \cdot d \tag{12}$$

where

d = length of path
I_0, I = intensity of excitation and fluorescence
ε = extinction coefficient
ϕ = quantum yield of fluorescence

These approaches are (1) determination of the amount of product continuously released by the bead as a measure of the total turnover rate, (2) determination of the radial intensity profiles, and (3) determination of the total product mass within the beads.

Total Turnover Rates

The total turnover rate of a single gel particle can be determined by integration of the individual rates at all points within the sphere volume. Since homogeneous enzyme distribution is assumed, the angular integration is independent of s, and hence the total turnover rate V_t becomes

$$V_t = k_1 R^3 V_m \int_0^1 \frac{s}{(1+\alpha s)[1+\alpha\beta(1-s)]} r^2\, dr \qquad (13)$$

The constant k_1 contains the factor 4π of the angular integration, the factor B (Eq. 11), and experimental factors. For the calculations k_1 was set = 1.

Total turnover rates of single spherical particles with immobilized enzymes have been calculated by Engasser and Horvath (11), though only for the uninhibited reaction and without experimental proof. Figure 3 shows the relative total turnover rates $V = V_t/V_m$ as a function of the substrate concentration α, with the Damköhler number σ as parameter. A double reciprocal plot (Figure 4) with R as parameter gives almost linear relations, as already described by Engasser and Horvath (11) and by Köstner (2). Only high substrate concentrations and high Damköhler numbers (e.g., high R)

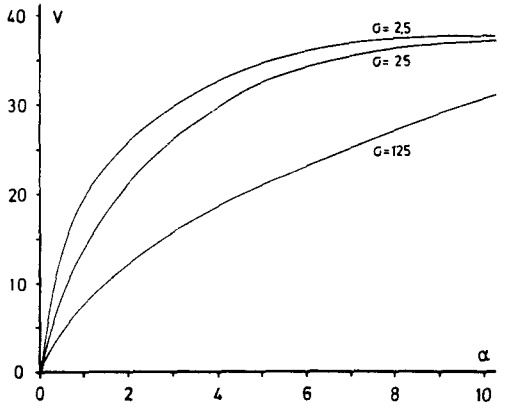

FIG. 3. Relative turnover rate V_t as a function of the substrate concentration α, with the Damköhler number σ as parameter.

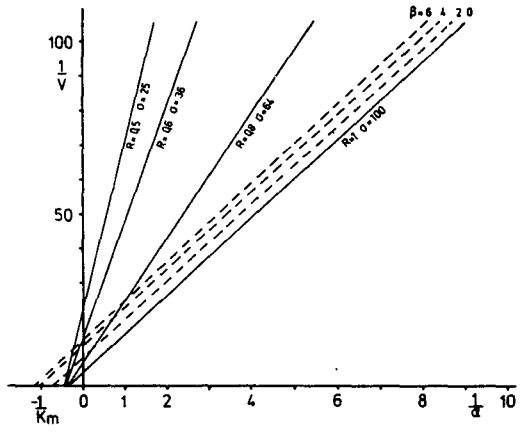

FIG. 4. Relative turnover rate V_i as a function of the substrate concentration α, with the radius R as parameter (———), and with increasing noncompetitive inhibition β at constant radius (– – –) (double reciprocal plot).

result in deviation from linearity, especially in an Eady-Hofstee plot (Figure 5). Noncompetitive product inhibition of the immobilized enzyme (Figure 4) gives rise to parallel shift in a Lineweaver-Burk plot, which would correspond to the behavior of an uncompetitive inhibition in a nondiffusion-limited, homogeneous enzyme reaction.

Intensity Profiles

Solution of Eq. (7) for the product, using Eq. (8), gives the stationary and radially symmetric product concentration profiles within the spheres ($0 < r < R$). These are not directly measurable, since microfluorometry can only measure concentrations integrated along the optical axis of the microscope over the thickness of the bead. Assuming an infinitely small measuring aperture for radial scanning of the fluorescent sphere, the measurable fluorescence intensity at any radial distance x is proportional to the integrated product concentration along the vertical path y at that point:

$$I(x) = k_2 \int_0^{(1-x^2)^{1/2}} p(r)\, dy \tag{14}$$

Since the coefficient k_2 again contains several parameters dependent on the experimental conditions, that is,

$$k_2 = 2 \cdot f(A, I_0, \phi, B, g) \tag{15}$$

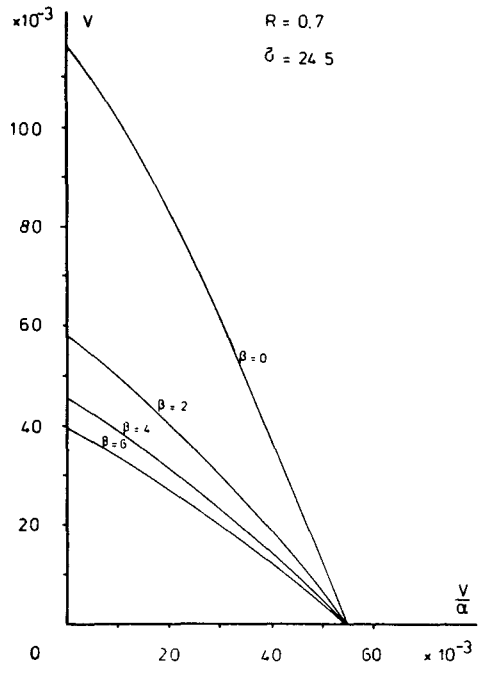

FIG. 5. Relative turnover rate V_t as a function of the substrate concentration α, with increasing inhibition β as parameter (plot according to Eady-Hofstee).

where A = aperture, I_0 = excitation intensity, ϕ = quantum efficiency, and g is a correction factor for the gel concentration, k_2 was set $=1$ for the calculations of relative intensity profiles. Figure 1 shows these calculated relative intensity profiles. It turned out that even over a high range of Damköhler numbers, $0.1 < \sigma < 100$, the differences between the profile shapes are relatively small.

Total Product Mass

The total product mass within the beads during steady-state turnover can be calculated from the product concentration integrated over the sphere volume:

$$I_t = k_3 R^3 K_m \int_0^1 p(r) r^2 dr \tag{16}$$

k_3 is equivalent to k_2 except for the geometric factor 4π. For the calculations it was set $k_3 \cdot K_m = 1$.

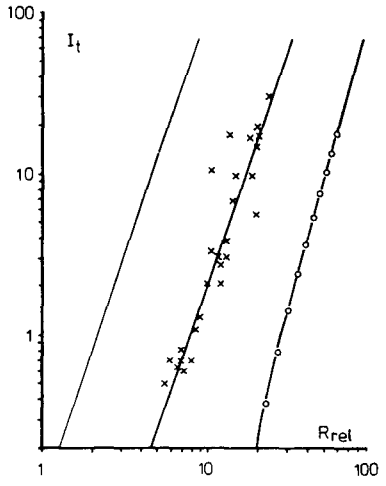

FIG. 6. Calculated total intensity I_t, (○), and experimental data as a function of the radius R_{rel} (double logarithmic plot with a straight line of slope 3 for comparison).

Figure 6 shows the total fluorescence intensity I_t as a function of the radius R_{rel}, i.e., R in arbitrary units, of the spheres in a double logarithmic plot. The dependence is approximately linear for the volume range plotted here, with slopes evidently higher than 3. For small σ and hence smaller R the slope becomes steeper, whereas for the case of extreme diffusional limitation, the slope reaches the value 3 asymptotically, and thus the intensities become volume-proportional in the case of absolute surface-restricted turnover.

Determination of the True K_m of the Immobilized Enzyme from Intensity- and Turnover-Dependent Apparent K_m's

Total intensities I_t and total turnover rates V_t are closely correlated, as is shown in Fig. 7. Therefore, a double reciprocal plot of $1/I_t$ vs. $1/\alpha$ gives almost linear dependency, by analogy to the graph of $1/V$ vs. $1/\alpha$ (Fig. 4). The case of noncompetitive product inhibition also yields parallel displacement toward lower total intensities, analogous to Fig. 4. From the double reciprocal plots of both measured total turnover rates $1/V$ vs. $1/\alpha$ (Fig. 4) and total intensities $1/I_t$ vs. $1/\alpha$, apparent Michaelis constants for different data sets of the diffusion-limited system can be defined as K_m^V and K_m^I by linear extrapolation to the intersection with the $1/\alpha$ axis, by analogy to homogeneous kinetics.

Figure 8 shows the dependence of these two types of apparent K_m's on the Damköhler number σ, with the inhibition constant β as parameter. In

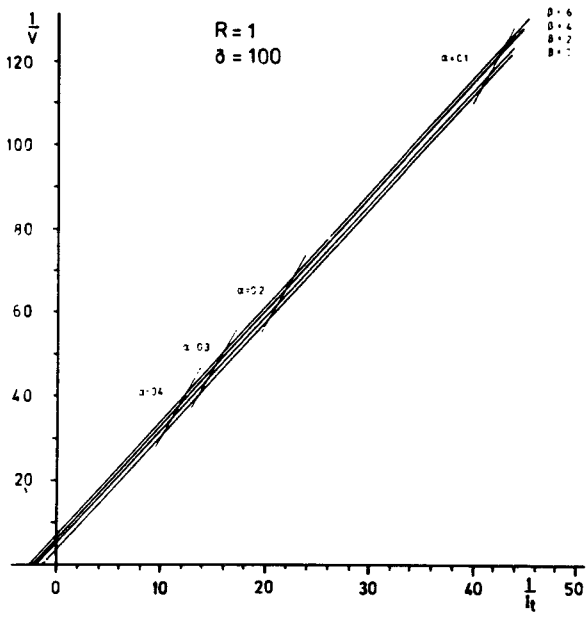

FIG. 7. Correlation between the total intensity I_t and the total turnover rate V_t, with inhibition β and substrate concentration α as parameters ($R = 1$, $\sigma = 100$) (double reciprocal plot).

both cases, extrapolation to $\sigma = 0$ would thus allow determination of the true Michaelis constant of the immobilized enzyme, if the apparent constants could be determined experimentally for a wide range of σ, for instance, by variation of R. Finally, the close correlation between V_t and I_t is valid also for the apparent Michaelis constants K_m^V and K_m^I, which are determined either from total intensities or total turnover rates (Fig. 9). Thus, if K_m^V and K_m^I can be determined simultaneously for spheres of different radii R with or without inhibition, it is possible on the basis of this plot of K_m^V/K_m vs. K_m^I/K_m to calculate the Damköhler number σ for single spheres.

Determination of the Effectiveness Factor η from the Relative Total Intensities

The effectiveness factor η is the ratio of the actual rate with diffusional limitation (V_t) to the maximum possible rate without diffusional limitation (V_0),

$$\eta = \frac{V_t}{V_0} \tag{17}$$

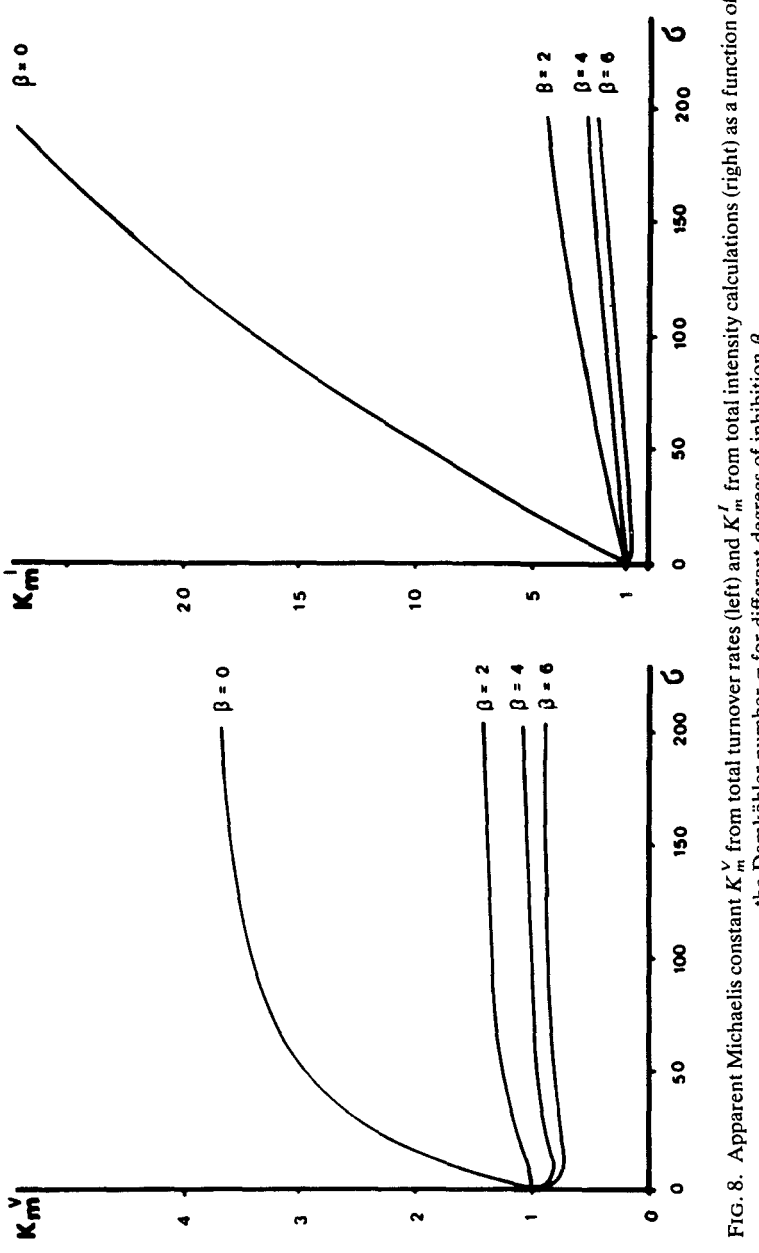

FIG. 8. Apparent Michaelis constant K_m^V from total turnover rates (left) and K_m^I from total intensity calculations (right) as a function of the Damköhler number σ for different degrees of inhibition β.

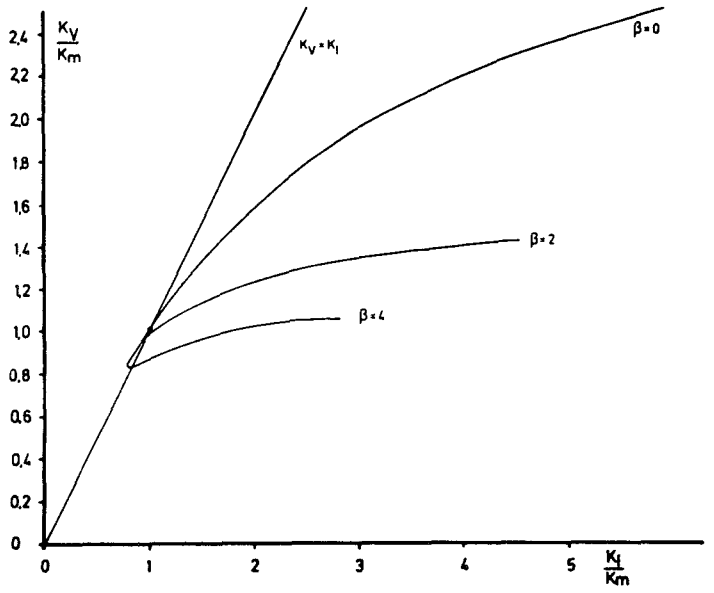

FIG. 9. Correlation of the apparent Michaelis constants K_m^V and K_m^I for determining the Damköhler number σ, without ($\beta = 0$) and with noncompetitive inhibition ($\beta = 2$ and $\beta = 4$).

Since V_0 represents the case $s(r) = 1$ for all r (see above), the maximum total rate can be calculated from Eq. (13):

$$V_0 = \frac{R^3}{3} \cdot \frac{\alpha}{\alpha + 1} \tag{18}$$

the effectiveness factor then becomes

$$\eta = 3(\alpha + 1) \int_0^1 \frac{s}{(1 + \alpha s)[1 + \alpha\beta(1 - s)]} r^2 \, dr \tag{19}$$

Figure 10 shows the effectiveness factor η as a function of the Damköhler number σ at different concentrations without and with noncompetitive product inhibition ($\beta = 4$). The appreciable decline of η with increasing σ and thus with increasing diffusional limitation is expressed by increasing noncompetitive product inhibition.

By analogy to the determination of the effectiveness factor from the ratio of the turnover rates, a corresponding measuring parameter can be determined from the ratio of the actual total intensity I of a sphere and the maximum possible total intensity I_{max} at a given substrate concentration:

$$I_{rel} = \frac{I}{I_{max}} \tag{20}$$

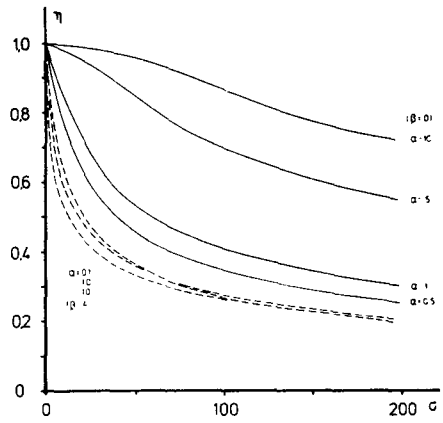

FIG. 10. Effectiveness factor η as a function of the Damköhler number σ, with the substrate concentration α as parameter, for the uninhibited case (———), and a case of noncompetitive inhibition ($\beta = 4$) (– – –).

The actual total intensity I from Eq. (16), with $K_m \cdot k_s = 1$, is

$$I = R^3 \alpha B \frac{D_s}{D_p} \int_0^1 (1-s) r^2 \, dr \tag{21}$$

Since the case of maximum total intensity is represented by $s(r) = 0$ for all r, we obtain

$$I_{\max} = \frac{R^3}{3} \alpha B \frac{D_s}{D_p} \tag{22}$$

and thus

$$I_{\text{rel}} = \frac{I}{I_{\max}} = 3 \int_0^1 (1-s) r^2 \, dr \tag{23}$$

Figure 11 shows these relative total intensities as a function of the Damköhler number σ with the substrate concentration as parameter, for cases without and with noncompetitive product inhibition ($\beta = 4$).

A comparison between the trends of the effectiveness factor as a function of σ (Fig. 10) and of the relative intensities I_{rel} evidently shows a reverse relation, while the validity and the sensitivity of these measuring parameters are identical. Their correlation is shown in Fig. 12 for different substrate concentrations. In contrast to the effectiveness factor η, the relative total intensities have the advantage of direct experimental access (see experimental results). They can be determined by comparing the total

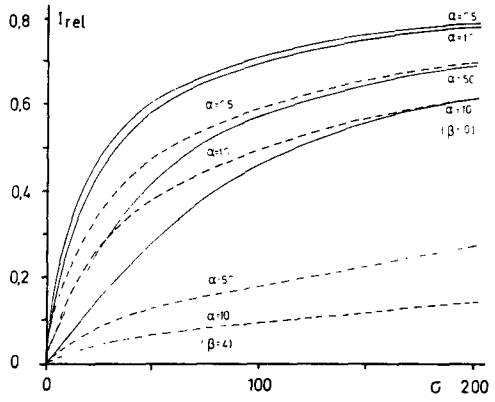

FIG. 11. Relative total intensity I_{rel} as a function of the Damköhler number σ for the uninhibited case (———) and a case of noncompetitive inhibition ($\beta = 4$) (– – –), with the substrate concentration α as parameter.

intensity of a sphere during steady-state turnover with the intensity of the same sphere emitted from a fluorescent product standard solution which has the same concentration as the substrate.

Experimental Results

To show the homogeneous distribution of bound enzyme within the gel matrix, the fluorescence I of FITC-esterase-Sepharose beads was measured as a function of the bead radius R. For statistical analysis, seven sets of data ($n \sim 30$) for enzyme loads ranging from 0.2 to 8.0 mg esterase per g Sepharose (9) were fitted to the function

$$I(R) = a\frac{4\pi}{3} \cdot R^b \tag{24}$$

where a is a measure of the staining intensity and b is a measure of the type of enzyme distribution. The fact that the calculated value of parameter b did not significantly differ from the value 3.0 allowed volume-proportional and thus homogeneous binding of the enzyme in the matrix to be assumed. The appreciable scatter in the case of log normal distribution of the intensities, on the other hand, is described by a factor of 1.58. It is not due to the noise of the fluorescence-proportional electric signal, but is to be attributed mainly to different densities of the beads due to inhomogeneous swelling of the freeze-dried CNBr-Sepharose matrix, whereas the single beads themselves are highly homogeneous, as had been proved by microinterferometry (7,9).

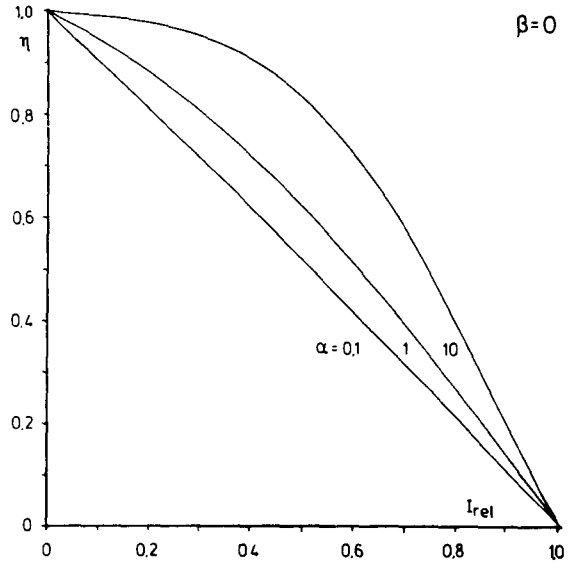

FIG. 12. Effectiveness factor η as a function of the relative total intensity I_{rel} ($\beta = 0$).

The scatter of gel concentration g between different beads was measured by microinterferometry according to the relation

$$g = \frac{\lambda}{\Delta n} \cdot \frac{w}{2R} \tag{25}$$

which, at given wavelength λ and refractive index difference Δn between matrix and solvent, is proportional to the interference fringe deviation w over the bead diameter $2R$ (Fig. 13). From this a standard deviation of 21.5% has been calculated for the relation $w/2R$, which can account for the wide scatter of the intensity measurements between different beads.

Another condition for the applicability of Eq. (7) and for the validity of effective diffusion constants is no or only concentration-proportional interaction between substrate or product and matrix. In order to determine the kind of interaction between fluorescein and the gel matrix, the fluorescence was measured as a function of the fluorescein concentration in the flow cuvette over a Sepharose 4B bead and over an esterase-Sepharose bead, and compared with the fluorescence of an equal volume between the beads (corrections for 4% gel volume were made). In both cases a linear increase of the intensity was observed up to 2×10^{-5} M fluorescein. The actual fluorescein concentration within the beads was increased by about 5.3% in the

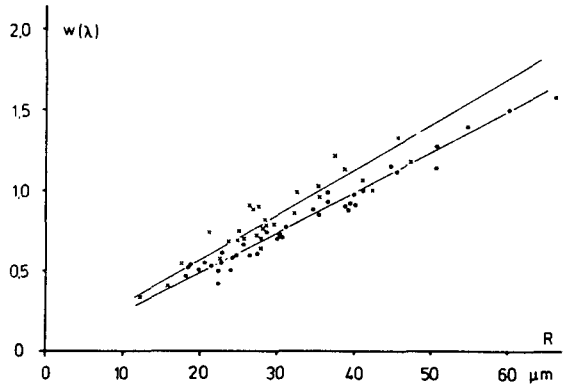

FIG. 13. Relative interference fringe deviation w over the center of a sphere as a function of the radius R of CNBr-Sepharose 4B beads (×, freeze dried sample; ○, non-freeze-dried sample).

Sepharose 4B matrix and by 9% in the esterase-Sepharose matrix (4 mg esterase per g Sepharose). The higher intensity in the case of esterase-Sepharose corresponds to unspecific binding of fluorescein to the esterase, as was also shown by the kinetic determination of noncompetitive product inhibition. Thus the validity of reversible, concentration-proportional binding was shown for fluorescein. For FDA, which cannot be measured optically, it can be assumed by analogy. Figures 6 and 14–16 show the results of determinations of the measurable kinetic parameters, proposed in the theoretical section above, for esterase-Sepharose beads.

Total Turnover Rates

The laminar thread of released product behind the spheres (7,9) is the only turnover-proportional parameter, which in our case, however, remains only a relative measure, since the actual flow velocity at this point in the cuvette is not easy to determine. Figure 14 presents the fluorescence over a defined part of the laminar product flow measured in a slit aperture as a function of the substrate concentration. A double reciprocal plot (according to Lineweaver and Burk) shows the theoretically predicted linear part of the relation (cf. Fig. 4), since due to the limited solubility no substrate concentration appreciably higher than the K_m was achieved.

A graphical method proposed by Engasser and Horvath (11) requires the determination of total turnover rates both at very high and low concentrations. Because of the restricted substrate solubility, the low intensities of the diluted product flow, and the wide scatter of the matrix properties, the

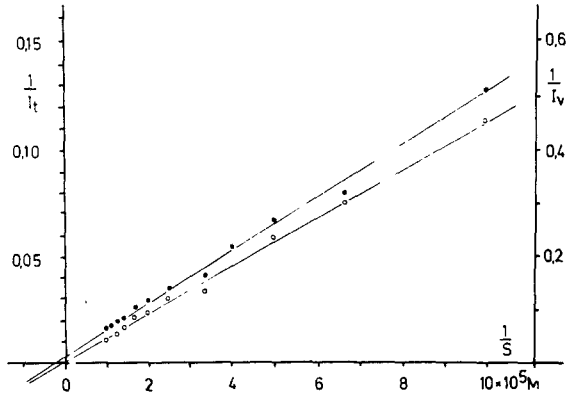

FIG. 14. Relative total turnover rate I_v, ○, and total intensity I_t, ●, of a single esterase-Sepharose bead as a function of the FDA concentration (double reciprocal plot).

accuracy necessary to determine the true K_m by this method has so far not been achieved by this procedure.

Intensity Profiles

Figure 15 shows the intensity profile of a sphere measured by scanning with a 1 μm^2 rectangular measuring diaphragm. The diameter of the diaphragm determines the radial resolution of the scan, but it competes with the intensity and thus the electric noise of the fluorescence signal. Therefore, a compromise between the two influences is necessary. Although the differences between the normalized profiles (Fig. 1) are relatively small, superposition of the experimental scan with a series of calculated profiles (Fig. 15) allows an estimate of the Damköhler number. In the special case shown, using the parameters $\alpha = 0.3$ and $\beta = 4.0$, the Damköhler number of this bead was determined to be in the range of $50 < \sigma < 70$. Absolute, not normalized, intensity profiles were found to be an even more sensitive measure of the system parameters. This, however, requires higher reproducibility of the microscopic stage positioning than could be achieved with the available equipment.

Total Intensity as a Function of Bead Diameter

Figure 6 shows the total intensities of single spheres at constant substrate concentrations as a function of the bead radius R in a double logarithmic plot. The slope of the regression line is nearly 3.0, corresponding to the case of extreme diffusional limitation, which was achieved at high

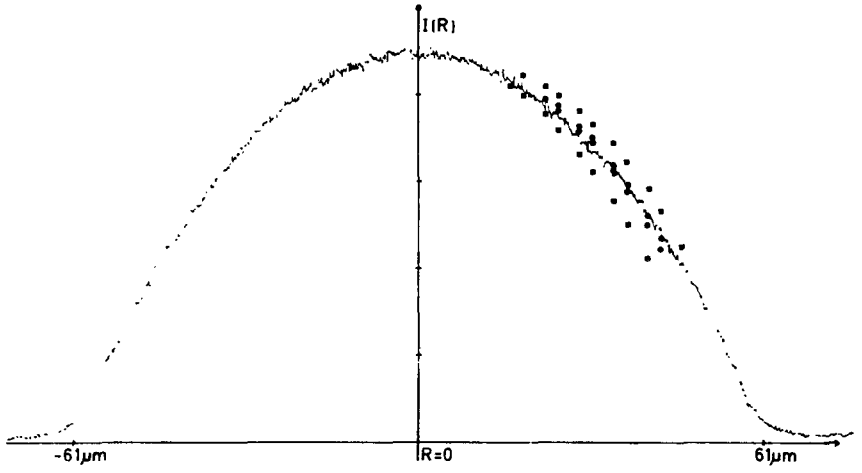

FIG. 15. Fluorescence intensity profile of a single esterase-Sepharose bead during turnover of 1×10^{-5} M FDA (measuring aperture 1 μm^2), with superimposed calculated intensity profiles (parameters $\alpha = 0.3$, $\beta = 4.0$, and $\sigma = 180$, ■, 70, ●, 50, ○, and 10, □) in the most sensitive radial range.

enzyme loads (about 20 mg esterase per g Sepharose). Previous total intensity determinations by Sernetz et al. (7) had already shown that slopes higher than 3 occur, which correspond to smaller values of σ. They can be related to either smaller R (Fig. 1) or smaller V_{max} [Eq. (10)] at lower enzyme content.

Total Intensity as a Function of Substrate Concentration

Figure 14 shows the total fluorescence intensity of a single esterase-Sepharose bead as a function of the substrate concentration in a double reciprocal plot. The linear relation in accordance with the theory allows the apparent K_m^I of single spheres to be determined. According to Fig. 8, extrapolation of these apparent K_m's of single spheres to the radius $R = 0$ (or $\sigma = 0$) should lead to the true K_m. This was attempted for spheres from the sample with 4 mg esterase per g Sepharose by plotting the individual K_m's vs. R^2 ($\sim\sigma$) of the spheres. The considerable scatter of the K_m^I is not to be attributed to errors in fluorescence measurements, but mainly to the unexpectedly high inhomogeneity of swelling and density of different spheres from the freeze-dried CNBr-Sepharose 4B sample (Fig. 13). Thus, in this respect the microfluorometric method could not be used in its full range. This limitation is assumed to be only preliminary, due to the inadequate properties of the material. It could be overcome, however, if gels

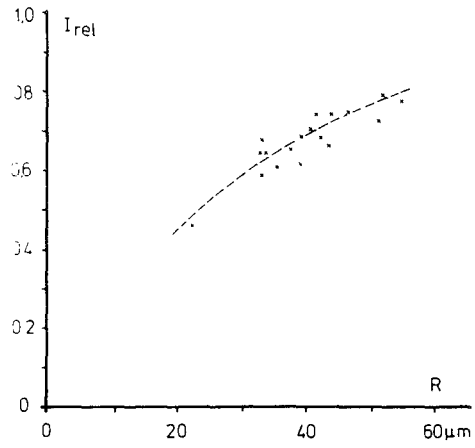

FIG. 16. Relative total intensity I_{rel} as a function of the radius R of single esterase-Sepharose beads.

of more homogeneous density become available. In addition, the error of graphical extrapolation could be reduced by raising the solubility of the fluorogenic substrate by chemical modification to values sufficiently above the K_m.

Relative Total Intensity

It has been pointed out (Fig. 12) that in theory the relative total intensity can serve as a parameter reciprocally related to the effectiveness factor η. The relative total intensity can be determined by comparison with the total intensity emitted from the same sphere volume of a standard solution of the fluorescent product having the same concentration as the substrate. For high enzyme loads (>8 mg esterase per g Sepharose), the total diffusional limitation was also determined in this way, as is shown in Fig. 6, from the volume proportionality of the intensities. Figure 16 shows the relative total intensities I_{rel} of single spheres, measured at 1×10^{-5} M FDA, corresponding to $\alpha \approx 1$, $\beta \approx 4$, as a function of the radius. With decreasing radius, the relative intensity also decreases, and thus the effectiveness factor becomes higher. As the scatter was again found to be due to the inhomogeneity of the matrix, a further evaluation was not meaningful at that point.

To make full use of the available precision of the fluorometric method for the determination of kinetic parameters, further investigations are aimed at improving the homogeneity of the matrix preparations and increasing the solubility of fluorogenic substrates for technically and biomedically relevant enzymes.

REFERENCES

1. LASCH, J. (1973) Mol. Cell. Biochem. 2:79.
2. KÖSTNER, A. (1973) Trudy Tallinskogo Politechničeskogo Instituta 331:157.
3. REGAN, D. L., LILLY, M. D., and DUNNILL, P. (1974) Biotech. Bioeng. 16:1081.
4. HORVATH, C. (1974) Biochim. Biophys. Acta 358:164.
5. LASCH, J., IWIG, M., and HANSON, H. (1972) Amer. J. Biochem. 27:431.
6. MOSBACH, K. (1971) Sci. Amer. 224:26.
7. SERNETZ, M., PUCHINGER, H., COUWENBERGS, C., and OSTWALD, M., Analyt. Biochem. 72 (1976) 24.
8. SERNETZ, M., and PUCHINGER, H. (1976) *In* Methods in Enzymology 44, Academic, New York, p. 373.
9. HANNIBAL-FRIEDRICH, O. (1977) Diss. Giessen (D 26).
10. ROTMAN, B., and PAPERMASTER, B. W. (1966) Biochemistry 55:134.
11. ENGASSER, J. M., and HORVATH, C. (1973) J. Theor. Biol. 41:137.
12. O'DRISCOLL, K. F. (1976) *In* Methods in Enzymology 44, Academic, New York, p. 169.
13. THIELE, E. W. (1939) Indust. Eng. Chem. 31:916.
14. ENGASSER, J. M., and HORVATH, C. (1974) Biochemistry 13:3845.
15. ENGASSER, J. M., and HORVATH, C. (1974) Biochemistry 13:3849.